ChemComm

COMMUNICATION

View Article Online
View Journal



Cite this: DOI: 10.1039/c5cc09161f

Received 4th November 2015,
Accepted 24th November 2015

DOI: 10.1039/c5cc09161f

www.rsc.org/chemcomm

# NAD-dependent dehydrogenase bioelectrocatalysis: the ability of a naphthoquinone redox polymer to regenerate NAD†

Sofiene Abdellaoui, Ross D. Milton, Timothy Quah and Shelley D. Minteer*

**Electron mediation between NAD-dependent enzymes using quinone moieties typically requires the use of a diaphorase as an intermediary enzyme. The ability for a naphthoquinone redox polymer to independently oxidize enzymatically-generated NADH is demonstrated for application to glucose/$O_2$ enzymatic fuel cells.**

Enzymatic fuel cells (EFCs) are devices that utilize enzymes at their anodes (and commonly at their cathodes) to facilitate the production of electrical energy from common energy-dense fuels, such as sugars and alcohols.[1–4] To date, high performance EFCs frequently incorporate flavin adenine dinucleotide-dependent (FAD) enzymes (*i.e.* FAD-dependent glucose dehydrogenase (FAD-GDH, E.C.: 1.1.99.10) and glucose oxidase (GOx, E.C.: 1.1.3.4)) commonly coupled to a single electron mediator; however, a large portion of EFCs make use of nicotinamide adenine dinucleotide-dependent (NAD) enzymes (*i.e.* NAD-dependent glucose dehydrogenase (NAD-GDH, E.C.: 1.1.1.47)).[5–9]

Alongside ferrocene[10–12] and osmium[13–16] electron mediators, quinones (typically naphthoquinones and anthraquinones) have been coupled with FAD- and NAD-dependent enzymes as efficient electron mediators, however an additional enzyme (diaphorase) is required as an intermediary between NAD-dependent enzymes and quinone electron mediators.[5,6,17]

*ortho*-Quinones have been reported to oxidize NADH, ranging from simple catechol derivatives to the enzymatic cofactor pyrroloquinoline quinone (PQQ).[18,19] Further, Katz *et al.* demonstrated the ability of an immobilized PQQ monolayer to efficiently oxidize NADH at gold and platinum electrode surfaces.[20] Another example is a ruthenium electron mediator recently published by Cosnier *et al.* that possessed a 9,10-phenanthraquinone ligand and was able to directly oxidize enzymatically-generated NADH.[21]

*Departments of Chemistry and Materials Science and Engineering, University of Utah, 315 S 1400 E, Room 2020, Salt Lake City, UT, 84112, USA. E-mail: minteer@chem.utah.edu*

† Electronic supplementary information (ESI) available: Experimental procedures, Fig. S1 (Michaelis–Menten kinetics). See DOI: 10.1039/c5cc09161f

While phenothiazines (such as methylene blue, methylene green, thionine and toluidine blue) are capable of oxidizing NADH without the need for diaphorase,[22–24] their immobilization by electropolymerization or covalent attachment to polymers results in a positive potential shift to less-desired onset potentials of NADH oxidation, due to the inherent change in chemical structure of the dye. Additionally, the purification of resulting phenothiazine polymers is not trivial whereby many polymers still possess entrapped non-covalently modified phenothiazine.

We recently reported a naphthoquinone redox polymer (NQ-LPEI) that was able to mediate electrons between FAD-GDH and yield an EFC with a remarkably high maximum current density (5.4 mA $cm^{-2}$) and maximum power density (2.3 mW $cm^{-2}$ at 0.55 V).[6] Herein, we report the ability of the NQ-LPEI redox polymer to directly oxidize enzymatically-generated NADH without the use of diaphorase. This NQ-LPEI redox polymer also offers additional benefits of low cost (compared to PQQ-based systems) and the ability to immobilize NAD-dependent enzymes within a 3-dimensional network. A glucose/$O_2$ EFC was constructed using NAD-GDH at the bioanode and laccase at the biocathode, yielding maximum current and power densities of 505.7 ± 56.7 μA $cm^{-2}$ and 123.2 ± 16.3 μW $cm^{-2}$ (respectively), with an associated OCP of 766.7 ± 4.9 mV.

Scheme 1 outlines the mechanism by which bioelectrocatalytic glucose oxidation by NAD-GDH is ultimately facilitated by the NQ redox polymer to the electrode surface. As previously reported, the NQ-LPEI redox polymer makes use of self-exchange (electron diffusion coefficient of $1.3 \times 10^{-11}$ $cm^2$ $s^{-1}$) to permit improved electron transport whereby the oxidation of NADH is not limited to a single adsorbed enzyme/mediator layer (such as that typically offered by π–π stacking architectures) but rather an expanded 3D electrode architecture.[6]

Fig. 1A presents cyclic voltammetry demonstrating the ability of the NQ-LPEI redox polymer to oxidize NADH, whereby NADH oxidation was initially investigated by the addition of reduced NADH to the citrate/phosphate buffer. It is important to demonstrate that the oxidation of NADH yields a biologically compatible $NAD^+$ cofactor, thus, the ability of the bioelectrode to oxidize

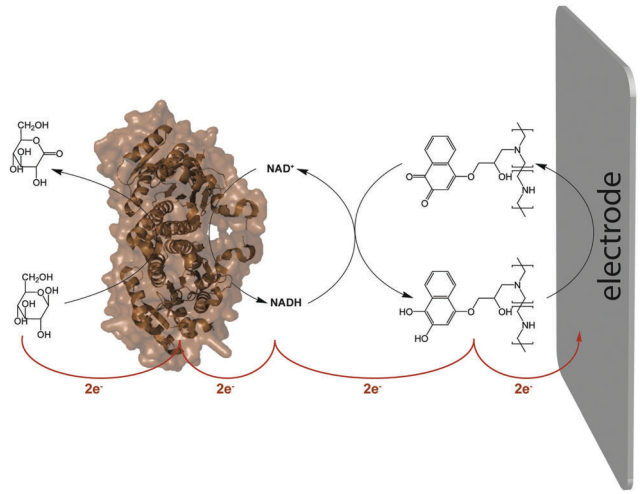


Scheme 1 Bioelectrocatalytic oxidation of glucose by NAD-dependent glucose dehydrogenase.

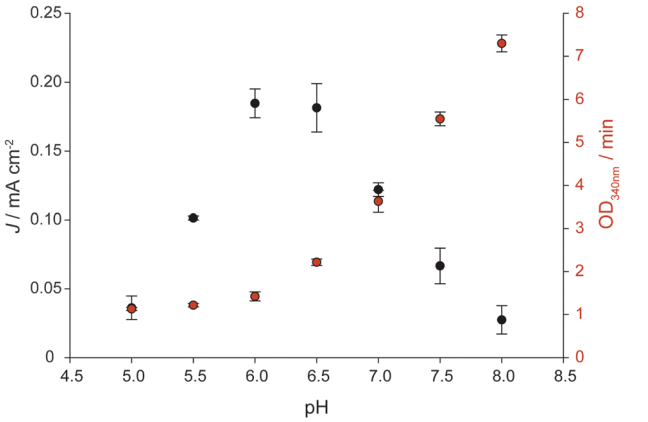


Fig. 2 Overlaid pH profile of electrocatalytic NADH oxidation (5 mM) at 0 V (*vs.* SCE) at NQ-LPEI/NAD-GDH bioelectrodes and NAD-GDH activities monitored by UV-Vis at 340 nm in presence of 5 mM $NAD^+$ and 100 mM glucose.

NADH generated from glucose oxidation by NAD-GDH was investigated (Fig. 1B). On Toray paper electrodes, a clear oxidative wave following the addition of glucose was observed. Control bioelectrodes comprised of an alternative LPEI-based polymer ($C_8$-LPEI, where the NQ moiety is replaced by a 8-carbon chain) and denatured NAD-GDH confirmed that the activity observed is in fact due to the enzymatic oxidation of glucose coupled to the enzymatic reduction of NADH (data not shown).

Enzymatic activity assays and cyclic voltammetry were employed to determine the optimal pH for glucose oxidation by NAD-GDH in a homogeneous setting and the optimal pH for NADH oxidation by the NQ-LPEI redox polymer, respectively (Fig. 2). Following electrochemical characterization was performed at pH 6.5, as a compromise between the alkaline optimal pH of glucose oxidation by NAD-GDH (as determined by UV-Vis experiments) and near-neutral NADH oxidation by the NQ-LPEI polymer.

Amperometric experiments were employed to determine the optimal concentration of $NAD^+$/NADH to be used with the NQ-LPEI/NAD-GDH bioelectrodes (Fig. 3A) at 0 V (*vs.* SCE at pH 6.5). The Michaelis–Menten model (by nonlinear regression) was employed in an attempt to evaluate the apparent kinetic parameters of NADH oxidation by the NQ-LPEI redox polymer and a control polymer ($C_8$-LPEI), on both glassy carbon and Toray paper electrodes. An apparent Michaelis constant ($K_M^{app}$) of 12.0 ± 0.6 mM NADH and a $J_{max}$ of 568.3 ± 14.6 μA $cm^{-2}$ were obtained for NQ-LPEI/NAD-GDH bioelectrodes on glassy carbon electrodes. The $K_M^{app}$ decreased to 4.3 ± 0.2 mM NADH when the bioelectrodes were scaled up to Toray paper, with an

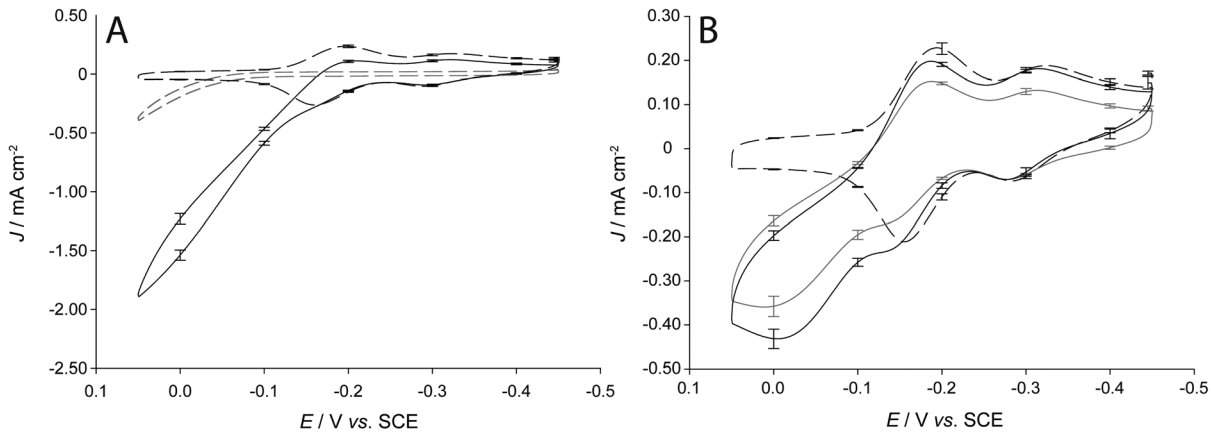


Fig. 1 (A) Representative cyclic voltammograms of NQ-LPEI/NAD-GDH bioelectrodes in citrate/phosphate buffer (0.2 M, pH 6.5) in the absence (black dashed line) and presence (black solid line) of 50 mM NADH, prepared on Toray paper electrodes (0.25 $cm^2$). Control bioelectrodes were prepared with $C_8$-LPEI/NAD-GDH (gray dashed line) in the presence of 50 mM NADH, on Toray paper electrodes. (B) Representative cyclic voltammograms of NQ-LPEI/NAD-GDH bioelectrodes in citrate/phosphate buffer (0.2 M, pH 6.5) containing 10 mM $NAD^+$, in the absence (black dashed line) and presence of 200 mM glucose (black solid line). Black lines represent bioelectrodes prepared on Toray paper, whereas the gray line represents electrodes prepared on glassy carbon electrodes. All electrodes were evaluated in hydrostatic quiescent buffer at a scan rate of 5 mV $s^{-1}$ ($n$ = 3, error bars represent one standard deviation).

 

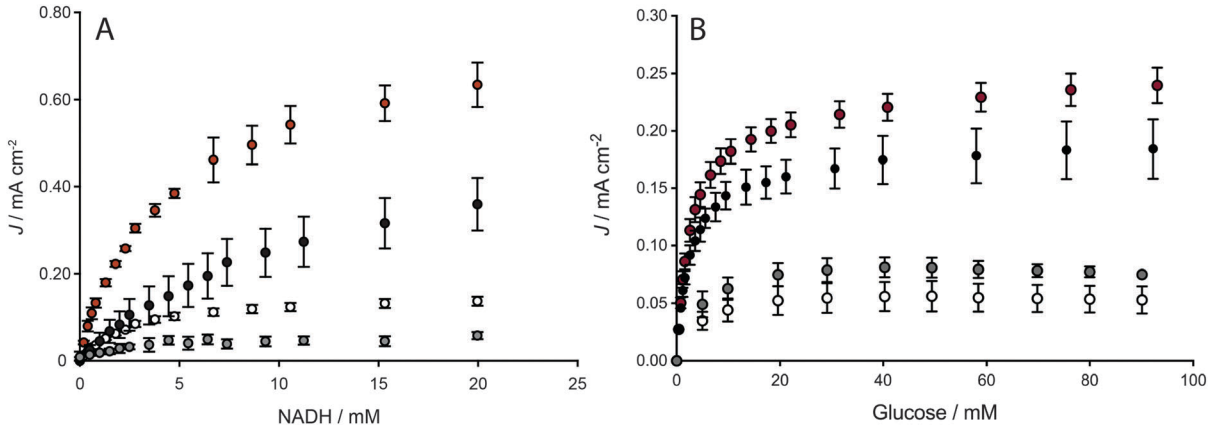


Fig. 3 (A) Calibration curve for the oxidation of NADH by the NQ-LPEI/NAD-GDH bioelectrodes at 0 V (*vs.* SCE). Bioelectrodes were prepared on glassy carbon (black) and Toray paper electrodes (red). Control bioelectrodes prepared with $C_8$-LPEI were evaluated on glassy carbon (gray) and Toray paper electrodes (white). (B) Apparent Michaelis–Menten kinetics for the bioelectrocatalytic oxidation of glucose by the NQ-LPEI/NAD-GDH bioelectrodes at 0 V (*vs.* SCE) in the presence of 10 mM $NAD^+$. Bioelectrodes were prepared on glassy carbon (black) and Toray paper electrodes (red). Control bioelectrodes prepared with $C_8$-LPEI were evaluated on glassy carbon (gray) and Toray paper electrodes (white). All electrodes were evaluated at in stirred citrate/phosphate buffer (0.2 M, pH 6.5) with no additional gas removal/purging ($n$ = 3, error bars represent one standard deviation).

increased $J_{max}$ of 756.9 ± 12.0 μA $cm^{-2}$. The decreased $K_M^{app}$ reflects an increase in affinity for NADH oxidation by the Toray paper bioelectrodes, also resulting in an increased $J_{max}$; thus, further electrochemical characterization was performed on Toray paper electrodes. Small contributions from the ability of the MWCNTs to electro-oxidize NADH (using the $C_8$-LPEI control polymer) result in a $J_{max}$ of 154.0 ± 1.4 μA $cm^{-2}$, which is approximately 20% of the catalytic current obtained for the NQ-LPEI redox polymer.

Since high concentrations of $NAD^+$/NADH are relatively costly, a concentration of 10 mM $NAD^+$ was selected for further evaluation. Control experiments were performed using a comparable LPEI-based polymer (absent of the NQ moiety, $C_8$-LPEI), on both glassy carbon and Toray paper electrodes.

Amperometric experiments were also used to evaluate the apparent enzymatic kinetics of the final NQ-LPEI/NAD-GDH bioelectrodes for glucose oxidation at 0 V (*vs.* SCE at pH 6.5, Fig. 3B). Apparent Michaelis–Menten kinetics were determined by non-linear regression and a $K_M^{app}$ of 3.0 ± 0.1 mM glucose was determined, with an associated $J_{max}$ of 238.5 ± 1.9 μA $cm^{-2}$, for NQ-LPEI/NAD-GDH bioelectrodes prepared on Toray paper electrodes. Interestingly, bioelectrodes prepared on glassy carbon electrodes had a $K_M^{app}$ of 2.7 ± 0.1 mM glucose, with an associated $J_{max}$ of 184.3 ± 1.5 μA $cm^{-2}$. Determination of the apparent Michaelis–Menten kinetics by Lineweaver–Burk double reciprocal linearization yielded a $K_M^{app}$ of 3.1 ± 0.1 mM glucose, with an associated $J_{max}$ of 244.0 ± 16.2 μA $cm^{-2}$.

UV-Vis experiments determined a comparable solution-based $K_M^{app}$ of 3.0 ± 0.2 mM glucose and a $V_{max}$ of 10.1 ± 0.1 mU, by following the production of NADH at 340 nm (Fig. S1, ESI†). Additional UV-Vis experiments were performed to confirm the ability of NQ to oxidize NADH, where the reduction of a

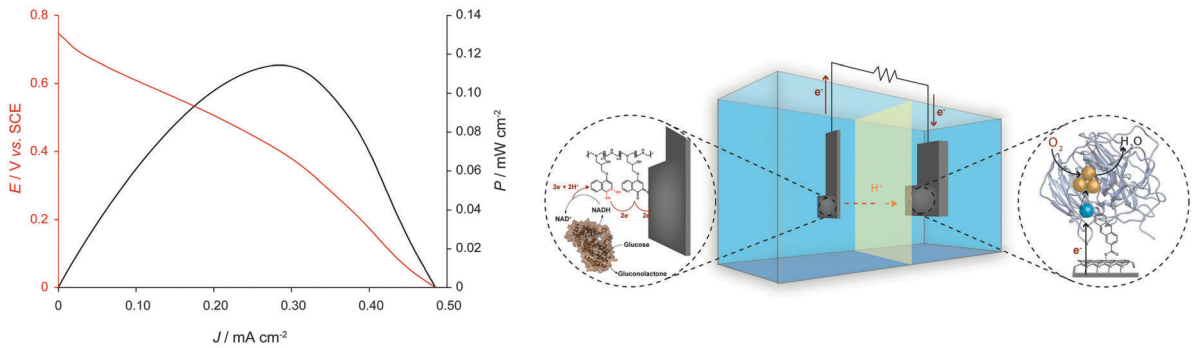


Fig. 4 Polarization and corresponding power curve for a glucose/$O_2$ EFC constructed using a NQ-LPEI/NAD-GDH bioanode coupled with a laccase DET-type biocathode. The EFC was operated using a proton exchange membrane to separate the anodic and cathodic chambers, to prevent the crossover and resulting oxidation of NADH at the biocathode. Thus, the anodic chamber consisted of citrate/phosphate buffer (0.2 M, pH 6.5) containing 200 mM glucose, whereas the cathodic chamber did not contain glucose (citrate/phosphate buffer, 0.2 M, pH 5.5). The anodic and cathodic chambers were stirred. Polarization was performed by galvanostatically drawing increasing current from the EFC at a slow sweep rate (0.1 μA $s^{-1}$), until short circuit. Current-limiting bioanodes were prepared on Toray paper electrodes with a geometric surface area of 0.25 $cm^2$, whereas biocathodes were prepared on Toray paper electrodes with a geometric surface area of 1 $cm^2$.

water-soluble naphthoquinone (1,2-naphthoquinone-4-sulfonic acid sodium salt) yielded a $K_M^{app}$ of 2.9 ± 0.1 mM glucose and a $V_{max}$ of 10.6 ± 0.1 mU (followed at 450 nm) (Fig. S1, ESI†). The similarities between the kinetics of the immobilized NAD-GDH and the solution based NAD-GDH reflect the limitation of the NAD-GDH on the bioelectrode by the concentration of NADH (as outlined above), resulting in a system that can be used to further study the enzymatic kinetics of NAD-dependent enzymes.

In light of high power EFCs that have been reported using NAD-dependent enzymes, the NAD-GDH bioelectrodes presented above were coupled with an enzymatic $O_2$-reducing biocathode to create a glucose/$O_2$ EFC (depicted in Fig. 3). The anodic and cathodic chambers were separated by a Nafion membrane separator to prevent crossover and competitive oxidation of NADH at the biocathode (ESI†). Laccase biocathodes were prepared with the use of anthracene-functionalized multi-walled carbon nanotubes (Ac-MWCNTs), whereby the anthracene moieties serve to orientate the T1 Cu centre of laccase and afford direct electron transfer (DET). The resulting laccase biocathodes are able to undergo a $4e^-$ reduction of $O_2$ to $H_2O$ without the need for an electron mediator (direct bioelectrocatalysis).[25] The construction of the laccase biocathodes is reported within the ESI,† of this manuscript.

Fig. 4 presents a polarization curve and corresponding power curve for a representative EFC; experiments were performed in triplicate. The EFCs possessed an OCP of 766.7 ± 4.9 mV, with associated maximum current and power densities of 505.7 ± 56.7 μA $cm^{-2}$ and 123.2 ± 16.3 μW $cm^{-2}$, respectively. Blank EFCs (tested in the absence of glucose) yielded approximate power densities of 17 μW $cm^{-2}$, produced as a function of the method used to evaluate the EFCs.

In conclusion, we demonstrate the ability of a naphthoquinone redox polymer to directly oxidize NADH in the absence of diaphorase, resulting in a simplified system. Resulting NAD-GDH bioelectrodes were utilized as glucose bioanodes with laccase $O_2$-reducing biocathodes in a glucose/$O_2$ EFC. It is anticipated that the system presented within this manuscript will impact a large number of NAD-dependent EFCs and cascade systems.

The authors thank the National Science Foundation and the Army Research Office MURI (#W911NF1410263) grant for funding. RDM acknowledges funding from a Marie Curie-Skłodowska Individual Fellowship (Global) under the EU Commission's Horizon 2020 framework (project number 654836).

## References

1 A. Heller, *Phys. Chem. Chem. Phys.*, 2004, **6**, 209–216.
2 S. D. Minteer, P. Atanassov, H. R. Luckarift and G. R. Johnson, *Mater. Today*, 2012, **15**, 166–173.
3 D. Leech, P. Kavanagh and W. Schuhmann, *Electrochim. Acta*, 2012, **84**, 223–234.
4 S. C. Barton, J. Gallaway and P. Atanassov, *Chem. Rev.*, 2004, **104**, 4867–4886.
5 H. Sakai, T. Nakagawa, Y. Tokita, T. Hatazawa, T. Ikeda, S. Tsujimura and K. Kano, *Energy Environ. Sci.*, 2009, **2**, 133–138.
6 R. D. Milton, D. P. Hickey, S. Abdellaoui, K. Lim, F. Wu, B. Tan and S. D. Minteer, *Chem. Sci.*, 2015, **6**, 4867–4875.
7 I. Osadebe and D. Leech, *ChemElectroChem*, 2014, **1**, 1988–1993.
8 B. Reuillard, A. Le Goff, C. Agnes, M. Holzinger, A. Zebda, C. Gondran, K. Elouarzaki and S. Cosnier, *Phys. Chem. Chem. Phys.*, 2013, **15**, 4892–4896.
9 Z. Zhu, T. Kin Tam, F. Sun, C. You and Y. H. Percival Zhang, *Nat. Commun.*, 2014, **5**, 3026.
10 D. P. Hickey, A. J. Halmes, D. W. Schmidtke and D. T. Glatzhofer, *Electrochim. Acta*, 2014, **149**, 252–257.
11 D. P. Hickey, F. Giroud, D. W. Schmidtke, D. T. Glatzhofer and S. D. Minteer, *ACS Catal.*, 2013, **3**, 2729–2737.
12 A. E. G. Cass, G. Davis, G. D. Francis, H. A. O. Hill, W. J. Aston, I. J. Higgins, E. V. Plotkin, L. D. L. Scott and A. P. F. Turner, *Anal. Chem.*, 1984, **56**, 667–671.
13 N. Mano, F. Mao and A. Heller, *J. Am. Chem. Soc.*, 2003, **125**, 6588–6594.
14 D. Macaodha, P. O. Conghaile, B. Egan, P. Kavanagh and D. Leech, *ChemPhysChem*, 2013, **14**, 2302–2307.
15 S. Tsujimura, K. Murata and W. Akatsuka, *J. Am. Chem. Soc.*, 2014, **136**, 14432–14437.
16 M. Shao, M. N. Zafar, M. Falk, R. Ludwig, C. Sygmund, C. K. Peterbauer, D. A. Guschin, D. MacAodha, P. O. Conghaile, D. Leech, M. D. Toscano, S. Shleev, W. Schuhmann and L. Gorton, *ChemPhysChem*, 2013, **14**, 2260–2269.
17 D. Fapyane, Y. Lee, C. Y. Lim, J.-H. Ahn, S.-W. Kim and I. S. Chang, *ChemElectroChem*, 2014, **1**, 1844–1848.
18 L. Gorton and E. Dominguez, *Rev. Mol. Biotechnol.*, 2002, **82**, 371–392.
19 L. Gorton, *J. Chem. Soc., Faraday Trans. 1*, 1986, **82**, 1245–1258.
20 E. Katz, T. Lötzbeyer, D. D. Schlereth, W. Schuhmann and H.-L. Schmidt, *J. Electroanal. Chem.*, 1994, **373**, 189–200.
21 B. Reuillard, A. Le Goff and S. Cosnier, *Anal. Chem.*, 2014, **86**, 4409–4415.
22 S. Pöller, M. Shao, C. Sygmund, R. Ludwig and W. Schuhmann, *Electrochim. Acta*, 2013, **110**, 152–158.
23 M. T. Meredith, F. Giroud and S. D. Minteer, *Electrochim. Acta*, 2012, **72**, 207–214.
24 Z. Huan, B. Persson, L. Gorton, S. Sahni, T. Skotheim and P. Bartlett, *Electroanalysis*, 1996, **8**, 575–581.
25 R. D. Milton, F. Giroud, A. E. Thumser, S. D. Minteer and R. C. T. Slade, *Chem. Commun.*, 2014, **50**, 94–96.

 